Title

Parathyroid hormone regulation of hypoxia-inducible factor signaling in osteoblastic cells

Authors

Wong, Alice
Loots, Gabriela G
Yellowley, Clare E
et al.

Publication Date

2015-12-01

DOI

10.1016/j.bone.2015.07.002

Peer reviewed

Published in final edited form as:

Bone. 2015 December ; 81: 97–103. doi:10.1016/j.bone.2015.07.002.

Parathyroid hormone regulation of hypoxia-inducible factor signaling in osteoblastic cells

Alice Wong[a], **Gabriela G. Loots**[b,c], **Clare E. Yellowley**[a], **Andréa C. Dosé**[a], and **Damian C. Genetos**[a,*]

[a]Department of Anatomy, Physiology, and Cell Biology, School of Veterinary Medicine, University of California, Davis, CA, USA

[b]Biology and Biotechnology Division, Lawrence Livermore National Laboratory, Livermore, CA, USA

[c]School of Natural Sciences, University of California, Merced, CA, USA

Abstract

Osteoblasts perceive and respond to changes in their pericellular environment, including biophysical signals and oxygen availability, to elicit an anabolic or catabolic response. Parathyroid hormone (PTH) affects each arm of skeletal remodeling, with net anabolic or catabolic effects dependent upon duration of exposure. Similarly, the capacity of osteoblastic cells to perceive pericellular oxygen has a profound effect on skeletal mass and architecture, as mice expressing stable hypoxia-inducible factor (HIF)-1α and -2α demonstrate age-dependent increases in bone volume per tissue volume and osteoblast number. Further, HIF levels and signaling can be influenced in an oxygen-independent manner. Because the cellular mechanisms involved in PTH regulation of the skeleton remain vague, we sought whether PTH could influence HIF-1α expression and HIF-α-driven luciferase activity independently of altered oxygen availability. Using UMR106.01 mature osteoblasts, we observed that 100 nM hPTH(1–34) decreased HIF-1α and HIF-responsive luciferase activity in a process involving heat shock protein 90 (Hsp90) and cyclic AMP but not intracellular calcium. Altering activity of the small GTPase RhoA and its effector kinase ROCK altered HIF-α-driven luciferase activity in the absence and presence of PTH. Taken together, these data introduce PTH as a regulator of oxygen-independent HIF-1α levels through a mechanism involving cyclic AMP, Hsp90, and the cytoskeleton.

Keywords

Hypoxia; Hsp90; Osteoblast; HIF; PTH; Cytoskeleton; Rho

*Corresponding author at: 1089 Veterinary Medicine Drive, Department of Anatomy, Physiology and Cell Biology, School of Veterinary Medicine, University of California Davis, Davis, CA 95616, USA. dgenetos@ucdavis.edu (D.C. Genetos).

Supplementary data to this article can be found online at http://dx.doi.org/10.1016/j.bone.2015.07.002.

1. Introduction

The mammalian skeleton undergoes continuous remodeling throughout its lifetime. This occurs in response to mechanical demands, the accumulation of microdamage within bone, and in response to hormonal factors like parathyroid hormone (PTH). PTH (Forteo™) remains the only current FDA-approved therapeutic agent that is skeletally anabolic when given intermittently; although extremely effective at mitigating senile osteoporosis [1], its use is limited to 18 months because of the emergent increased risk of osteosarcoma and other skeletal neoplasms documented in rodent models treated for longer periods. PTH binding to its cognate receptor activates distinct Gα subunits to synthesize cyclic AMP, activate phospholipase C to cause release of calcium from intracellular stores, and disrupt the actin cytoskeleton [2,3]. Each of these signaling pathways is implicated in mediating osteoblast mechanosensitivity [4,5], and the anabolic and catabolic effects of PTH on the skeleton [6].

The cells that form tissues and organs and comprise an organism demonstrate a remarkable capacity to respond to changes in their extracellular milieu, enabling them, and ultimately the whole organism, to adapt to altered nutritional, biophysical or other conditions. For example, cells and tissues must adapt to changes in oxygen bioavailability arising from physiological or pathological conditions. Adaptive responses to decreased oxygen tension (hypoxia) are rectified by the transcriptional induction of genes that promote angiogenesis and anaerobic glycolysis, a phenomenon mediated in part by the hypoxia-inducible factor (HIF) family of transcription factors [7]. Constitutively expressed HIF-1β (also arylhydrocarbon receptor nuclear translocator, ARNT) binds to one of the three distinct HIF-alpha isoforms (HIF-1α, HIF-2α, and HIF-3α) to initiate gene expression. Oxygen levels regulate HIF-responsive gene expression. Under normoxic conditions, HIF alpha subunits are hydroyxlated by proline hydroxylase-domain proteins (PHDs), targeted for ubiquitination by the E3 ligase complex von Hippel–Landau (Vhl) and are ultimately degraded by the 26*S* proteasome. Under hypoxic conditions, prolyl hydroxylation of HIF-α is inhibited, enabling HIF-α levels to accumulate, translocate into the nucleus, complex with HIF-β/ARNT, and finally bind to HIF-response elements (HRE) within target genes.

During embryonic development, endochondral bone formation is accompanied by vascular invasion of the cartilaginous anlage. Inhibition of angiogenic growth factor VEGF with a decoy receptor prevents vessel invasion and trabecular bone growth [8]. The interdependence between osteogenesis and angiogenesis is further supported by tissue engineering approaches, wherein the combination of angiogenic and osteogenic factors increase in vivo bone formation compared to delivery of either factor alone [9]. Deletion of *Vhl* in osteoblasts and osteocytes constitutively stabilizes HIF-1α and -2α, increases VEGF expression, endothelial sprouting, and enhances long bone volume, bone formation rate, and osteoblast number [10]. Similarly, deletion of HIF-1α and -2α in osteoblasts and osteocytes exerts distinct and overlapping effects on the skeleton: HIF-1αdeletion decreases trabecular bone volume, mineral apposition rate, and proliferation, whereas both HIF-1α and -2α contribute to vessel number and volume and hypoxic induction of *Vegf* [11]. Thus, regulation of HIF signaling has direct effects on the skeleton.

In addition to the well-characterized oxygen-dependent regulation of HIF-α members, mammalian cells also demonstrate the capacity for oxygen-independent regulation of HIF stability and signaling. Insulin and IGF-I increase HIF-1α protein levels through PI3K/mTOR [12,13] without altering expression of endogenous inhibitors of HIF-α stability [13], although there are contradictory reports on whether IGF-I directly affects HIF-1α mRNA levels [13,14]. Additionally, heat shock protein 90 (Hsp90) serves as an endogenous oxygen-independent stabilizer of HIF-1α protein levels: competition between binding of HIF-1α by Hsp90 versus receptor for activated C-kinase 1 (RACK1) influences HIF-1α presentation to ElonginC and its subsequent oxygen-independent degradation [15,16].

Since the cellular mechanisms whereby PTH exerts anabolic or catabolic effects remain unknown and because of emerging interest in the role of HIF in bone, we examined the influence of PTH on HIF signaling, in osteoblasts. Here, we demonstrate that PTH inhibits HIF-1α protein levels under normoxic conditions, and decreases HIF-dependent signaling. This process is mimicked with the Hsp90 antagonist geldanamycin, involves cyclic AMP, and requires RhoA function. These results attribute a novel function for PTH in oxygen-independent regulation of HIF-1α.

2. Materials and methods

2.1. Materials

Human PTH(1–34), human PTH(1–31), and bovine PTH(3–34) were purchased from Bachem, reconstituted at 100 μM stock, aliquoted and frozen at −80 °C. The Rho inhibitor exoenzyme C3 transferase and the Rho Activator II (CN-03) were each purchased from Cytoskeleton. 8-bromo-cAMP was from Calbiochem, and geldanamycin was from Sigma.

2.2. Cell culture

UMR106.01 mature osteoblasts [17] (kindly provided by Dr. Alexander G. Robling, Indiana University School of Medicine) were cultured in MEM with Earle's Salts (*Invitrogen*) supplemented with 10% fetal bovine serum (FBS; Invitrogen) and 1% penicillin and streptomycin (P&S; Invitrogen). Cells were maintained in a standard humidified incubator at 37 °C with a 95% air and 5% CO_2 environment, and were routinely sub-cultured when 70–80% confluent with 0.05% trypsin (Gibco Life Technology).

2.3. Transient transfections and luciferase assays

A pGL3-HIF reporter element (pVEGF-Luc) vector driving expression of firefly luciferase (*Photinus pyralid*), containing the promoter region of human vascular endothelial growth factor (hVEGF) from −1005 to +379, was used as described previously [18]. Alternately, a firefly luciferase plasmid containing three hypoxia response elements from the *Pgk1* gene was used; pPGK1-luciferase was a gift from Dr. Navdeep Chandel (Addgene plasmid #26731, [19]). Renilla luciferase, under control of the thymidine kinase promoter (pRL-TK; Promega), was co-transfected as a control for transfection efficiency. Cells were seeded at 20,000 cells/well in 48-well plates and transfected the next day in Opti-MEM with 300 ng pVEGF-Luc or pPGK1-Luc, 300 ng pRL-TK, and 1.2 μL of X-TremeGENE HD(Roche). Reagents were added the following day, and wells were collected in 50 μL passive-lysis

buffer 24 h later unless otherwise indicated. Luciferase activity in recovered lysates was determined using the Dual-Luciferase Reporter Assay System (Promega) and a Turner Designs Model 20/20 Luminometer. Within each sample, firefly luciferase activity was normalized to pRL-TK to compensate for potential variations in transfection efficiency or cell number. For transfection of RhoA mutants, GFP-RhoA was a gift from Dr. Channing Der (Addgene plasmid #23224, [20]), while dominant negative pRK5-myc-RhoA-T19N (Addgene #12963, unpublished) and constitutively active pcDNA3-EGFP-RhoA-Q63L (Addgene plasmid #12968, [21]) were gifts from Dr. Gary Bokoch (The Scripps Research Institute); cells were seeded and transfected as described above.

2.4. Site-directed mutagenesis of pPGK1-Luc

Inverse PCR was performed to generate the HRE-deleted pPGK1-Luc plasmid. The following phosphorylated primers were used in a 50 μL reaction with PFU turbo (Strategene): (F) 5′-AGCTCGAGATCCGGCCCC-3′; (R) 5′-ACAGAGCTCGGTACCTCCC-3′. Following 24 cycles of PCR, the product was digested with *DpnI*, ligated and transformed into DH5alpha competent cells (Life Technologies). Mini-prep of colonies, followed by PCR, identified deletion mutants (249 bp vs 320 bp for wildtype plasmid) which were confirmed by sequencing. The following primers were used for deletion identification and sequencing: (F) 5′-GCATTCTAGTTGTGGTTTGTCC-3′; (R) 5′-ACGCTGTTGACGCTGTTAAGC-3′.

2.5. Western immunoblotting

For protein analysis, samples were cultured as described above and lysed in 0.1% Triton X-100, 10 mM Tris–HCl, pH 8, 1 mM EDTA, supplemented with a protease and phosphatase inhibitor cocktail (Pierce-ThermoFisher). Samples were resolved in 10% Bis–Tris gels (Invitrogen), transferred onto 0.2 μm nitrocellulose membranes, and blocked in non-fat milk in a Tris-buffered saline supplemented with 0.1% Tween-20. Antibodies against HIF-1α (Millipore) and Hsp90 (Cell Signaling) and α-tubulin (Cell Signaling) were added at recommended concentrations overnight, then probed at room temperature with appropriate horseradish peroxidase-conjugated secondary antibodies (Jackson Immunoresearch). Immunoreactive bands were visualized using enhanced chemiluminescence (Bio-Rad) and a ChemiDoc MP Imaging System (Bio-Rad).

2.6. Statistical analysis

Each experiment consisted of a minimum of 3 independent trials, with each independent trial composed of samples in triplicate or quadruplicate. Unless otherwise noted, Luciferase data were normalized to internal control pRL-TK, and then to vehicle control to account day-to-day transfection variability, and are presented as mean +/− SEM. Immunoreactive bands for western blotting were normalized to internal control α-tubulin, and then to vehicle. Statistical significance was assessed by two-tailed Student's *t* test or ANOVA for non-repeated measurements followed by a Dunnett post-hoc analysis compared to vehicle control. A $p < 0.05$ was considered statistically significant. Statistically similar columns are noted with the same letters whereas statistically distinct columns are denoted by different letters.

3. Results

3.1. Parathyroid hormone decreases O_2-independent HIF signaling

To determine whether PTH could regulate HIF expression and signaling, mature osteoblastic cells (UMR106.01) were transfected with a HIF reporter plasmid (pVEGF-Luc) driving expression of firefly luciferase and reporter activity was examined as a function of PTH treatment. Cells treated with 100 nM hPTH(1–34) for 6 or 24 h demonstrated a ~45% reduction in luciferase activity ($p < 0.003$) compared to vehicle controls (Fig. 1A). The magnitudes of pVEGF-Luc suppression were similar after 6 and 24 h of treatment, and were not statistically different ($p < 0.75$) from each other. PTH-induced decreases in pVEGF-Luc activity corresponded to a decrease in HIF-1α levels, as determined by western immunoblotting, (Fig. 1B), wherein a similar magnitude suppression of pVEGF-Luc and HIF-1α protein was observed in response to 24 h treatment with hPTH(1–34). To determine the persistence of pVEGF-Luc suppression by PTH, cells were treated with hPTH(1–34) for 0, 2, 4, or 24 h, and allowed to recover in PTH-free media, for a total of 24 h. Treatment with hPTH(1–34) for 4 h followed by recovery for 20 h demonstrated similar reductions in pVEGF-Luc as cells that received continuous hPTH(1–34) for 24 h (Fig. 1C), whereas cells treated with PTH for 2 h followed by 22 h recovery showed no statistically significant difference in pVEGF-Luc compared to vehicle treated controls. These data indicate that the duration of PTH signaling determines the persistence of pVEGF-Luc suppression. From these results, we conclude that the influence of PTH on HIF is rapid and sustained, suggesting that modest perturbations in HIF signaling may be permissive for cells to respond to other HIF-altering stimuli.

To evaluate whether our choice of promoter influenced the results described above, UMR106.01 osteoblasts were transfected with an alternate luciferase reporter plasmid containing three copies of HRE from the *Pgk1* gene [19]; similar suppressive effects of hPTH(1–34) on luciferase activity were observed in pPGK1-Luc, indicating that choice of promoter did not influence the suppressive effect of hPTH(1–34) on HIF-α signaling (Fig. 2A). To further confirm specificity, site-directed mutagenesis of HRE elements within pPGK1-Luc was employed. Clones resolved on agarose gel at expected molecular weight (320 bp for wild-type vs 249 bp for mutant HRE; Fig. 2B), and failed to decrease luciferase activity in response to hPTH(1–34) compared to parental plasmid (Fig. 2C). These data confirm that the capacity of hPTH(1–34) to decrease HIF-α signaling is not dependent on the plasmid choice.

Whereas HIF signaling has been traditionally evaluated in the context of oxygen bioavailability (i.e., oxygen-dependent regulation), HIF can also be regulated through oxygen-independent mechanisms, wherein HIF binding to the molecular chaperone Hsp90 prevents its degradation through an oxygen-independent E3 ubiquitin ligase [22]. To determine if the same oxygen-independent mechanism occurs in mature osteoblasts, UMR106.01 cells transfected with pVEGF-Luc were treated with the Hsp90 antagonist geldanamycin (0–1 μM) [23] for 24 h. We observed dose-dependent inhibition of pVEGF-Luc activity in response to geldanamycin (IC_{50} = 15.7 nM; Supplemental data). Cells co-treated with hPTH(1–34) and geldanamycin did synergistically suppress pVEGF-Luc

activity (Fig. 3A), suggesting that PTH decreases HIF-α through an Hsp90-mediatedmechanism. hPTH(1–34) decreased Hsp90 protein levels, as determined by quantification of immunoreactive Hsp90 in control or hPTH(1–34)-treated UMR106.01 osteoblasts (Fig. 3B), and HIF-1α and Hsp90 protein levels demonstrated a strong positive correlation in the absence and presence of PTH (Pearson correlation r = 0.897; $p < 0.0002$; Supplemental data). These data suggest that PTH exerts inhibitory effects on pVEGF-Luc through regulation of Hsp90.

3.2. PTH decreases pVEGF-Luc through cyclic AMP-dependent mechanisms

PTH exerts cellular responses through the activation of cAMP/PKA-and/or Ca^{2+}/protein kinase C-mediated signaling. hPTH(1–34) mimics the effect of full-length PTH(1–84), and its amino-terminal fragment hPTH(1–31) activates cAMP/PKA with little effect on PKC [24], while bPTH(3–34) activates Ca^{2+}/PKC signaling without stimulating cAMP/PKA [24]. Thus, use of hPTH(1–31) and bPTH(3–34) enables selective activation of cAMP/PKA versus Ca^{2+}/PKC signaling in order to examine the individual contribution of these signaling pathways on PTH(1–34)-dependent pVEGF-Luc suppression. Treatment with 100 nM hPTH(1–34) or hPTH(1–31) each decreased pVEGF-Luc by 50% (Fig. 4A), and there was no statistical difference in effect between hPTH(1–34) and hPTH(1–31) ($p > 0.999$); in contrast, bPTH(3–34) failed to alter pVEGF-Luc activity compared to control. These data suggest that PTH exerts inhibitory effects on pVEGF-Luc through cAMP/PKA and not Ca^{2+}/PKC. Involvement of PKA was also tested using the membrane-permeant cAMP analog 8-bromo-cAMP (1 mM), which mimicked the effect of hPTH(1–34) on pVEGF-Luc by decreasing luciferase activity by 63% (Fig. 4B), and there was no statistical difference in pVEGF-Luc reduction in response to hPTH(1–34) versus 8-bromo-cAMP ($p > 0.90$).

3.3. PTH regulates HIF-driven signaling through RhoA/ROCK

PTH exerts diverse effects in osteoblasts that ultimately lead to protein expression required for bone formation. In addition to altering cytosolic levels of the second messengers, PTH rapidly disrupts the actin cytoskeleton and reduces stress fibers through a cAMP-dependent mechanism. Having observed that reductions in pVEGF-Luc activity are mediated through cAMP, we next examined the involvement of the small GTP-binding protein RhoA, the activation of which promotes stress fiber formation, in PTH-mediated pVEGF-Luc suppression. Direct activation of RhoA with a cell-permeant agonist Rho Activator II (1 or 2.5 μg/mL) increased pVEGF-Luc activity, and this was attenuated by co-treatment with hPTH(1–34) (Fig. 5A). Lysophosphatidic acid, a known activator of RhoA, dose-dependently increased pVEGF-Luc activity (Supplemental data), and the LPA receptor 1/3 antagonist Ki16425 (10 or 20 μM) significantly attenuated basal pVEGF-Luc activity (Supplemental data). Co-treatment of cells with 100 nM hPTH(1–34) and 100 μM LPA reduced pVEGF-Luc similar to LPA-free controls (Fig. 5B), as did co-treatment of cells with 100 μM LPA and the RhoA inhibitor exoenzyme C3 transferase (Fig. 5C). To further corroborate these results, we next transfected cells with EGFP-pcDNA or EGFP-Rho mutant plasmids, where EGFP-RhoA-T19N expresses dominant negative RhoA, and EGFP-RhoA-Q63L expresses constitutively active RhoA. We again observed reductions in pVEGF-Luc in response to hPTH(1–34) in cells transfected with control EGFP-pcDNA, but co-expression of dominant negative EGFP-RhoA-T19N showed no effect of PTH(1–34) on

pVEGF-Luc, while cells transfected with constitutively-active EGFP-RhoA-Q63L lose the suppressive effect of PTH on pVEGF-Luc (Fig. 5D). These data indicate that RhoA is crucial for PTH-induced suppression of pVEGF-Luc.

4. Discussion

Herein, we demonstrate a novel function for parathyroid hormone in osteoblastic cells. Because PTH remains the only FDA-approved osteoanabolic therapeutic agent to date, and because there are drastic anabolic or catabolic differences in skeletal response that is dependent on mode of PTH administration, ongoing examination of the mechanism of PTH action is necessary. Using two different HIF-1αresponse element (HRE)-containing luciferase expression plasmids and UMR106.01 mature osteoblasts, we found that hPTH(1–34) decreases pVEGF-Luc and pPGK1-Luc activity in a rapid and sustained fashion; western immunoblotting also demonstrated decreased HIF-1α protein levels in response to hPTH(1–34). Mechanistic examinations of oxygen-independent regulation of HIF-1α by PTH indicate involvement of cAMP, the chaperone protein Hsp90, and RhoA-ROCK signaling.

Initial discoveries indicated that HIF-1α protein is regulated as a function of pericellular oxygen tension [25]. Oxygen-dependent regulation of HIF-1α involves its hydroxylation at proline residues 402 and 564 by PHDs, which facilitates HIF-1αbinding to Vhl, HIF-1αpolyubiquitination, and ultimately proteasomal degradation. As pericellular oxygen bioavailability decreases, PHDs cannot hydroxylate HIF-1α, which escapes binding to Vhl and polyubiquitination, resulting in increased HIF-1α-driven gene expression. Research in the last decade has demonstrated the existence of that multiple oxygen-independent means to control HIF-1α protein expression and HIF-1α-driven gene expression. The chaper-one Hsp90 stabilizes HIF-1α protein [22] by preventing HIF-1α binding to RACK1. RACK1 serves as a multifunctional scaffolding protein involving the ElonginC/ElonginB E3 ubiquitin ligase complex to promote HIF-1α ubiquitination in an oxygen-, hydroxylation-, and Vhl-independent manner. Both Hsp90 and RACK1 compete for binding to amino acids 81–200 in HIF-1α, a region containing the PAS-A subdomain critical for HIF-1α and -1β subunit heterodimerization and DNA binding, such that HIF-1α levels independent of oxygen are balanced between its binding to Hsp90 versus RACK1. Disruption of Hsp90/HIF-1α interaction, due to siRNA or chemical antagonists, promotes HIF-1α ubiquitination and proteasomal degradation, thereby decreasing HIF-1α transcriptional activity [22]; in contrast, RACK1 shRNA [15] or Hsp90 over-expression [26] increases HIF-1α accumulation and HIF-1α-driven gene expression under normoxic conditions. While we did not examine the influence of RACK1 in PTH-regulated HIF-1α expression, we observed that inhibition of Hsp90 with geldanamycin decreased pVEGF-Luc (Supplemental data) and Hsp90 expression (Fig. 3B) in a dose-dependent manner. Our data suggest that PTH requires reductions in Hsp90 in order to elicit effects on pVEGF-Luc and HIF-1α levels, as there was no synergistic effect of 100 nM hPTH(1–34) and geldanamycin on pVEGF-Luc activity (Fig. 2B), especially at geldanamycin concentrations above its calculated IC_{50} of 15.7 nM.

One of the observed effects of PTH on osteoblastic and osteocytic cells is disruption of the actin cytoskeleton. PTH rapidly and dose-dependently decreases actin and myosin content of

Triton X-100-insoluble cell lysates [3], a process that appears to be mediated via cyclic AMP, rather than Ca^{2+} [3,27]. cAMP-induced morphological changes may be counteracted by RhoA and ROCK-II, as constitutively active RhoA-G14V prevented morphological changes in response to the cAMP-mobilizing agent forskolin [28]. These, and other findings, suggest a generalized, if not facile, view of stress fiber formation as a balance between cAMP and Ca^{2+}, wherein Ca^{2+} activation of MLCK promotes MLC contraction and stress fiber formation, versus cAMP activation of MLC phosphatases and inhibition of RhoA promotes disassembly. We observed that activation of cAMP signaling, either with PTH(1–31) (Fig. 4A) or 8-br-cAMP (Fig. 3B), mimics the effect of PTH(1–34), suggesting that the capacity for PTH to decrease pVEGF-Luc pVEGF-Luc activity is dependent upon cAMP, and not Ca^{2+}, as PTH(3–34) had no effect on pVEGF-Luc signal.

Previous reports revealed that PTH effects on Rho and ROCK in osteoblastic cells, as PTH-induced PKCα translocation [29] and phospholipase D [30] through Rho-dependent mechanisms, and PTH was found to increase GTP-bound RhoA [29]. Our results demonstrate the opposite, that PTH decreases RhoA activation. Perhaps these differences are due to the signaling cascades activated, as PTH(3–34), which activates Ca^{2+}/PKC signaling, mimicked the effect of PTH(1–34) in these studies [29], whereas in our studies cAMP and PTH(1–34) elicited the same effect as PTH(1–34) (Fig. 3A and B). However, that PTH activates RhoA is at odds with the observed effect of each of these agents individually on actin stress fiber formation in osteoblasts: PTH decreases, and RhoA activation increases, stress fiber formation. Further, inhibiting Rho function by preventing its geranylgeranylation or its effector kinase ROCK in otherwise untreated cells causes loss of actin stress fibers and reductions in focal adhesions [31]. Thus, more investigation is required to delineate the effect of PTH-induced cAMP or Ca^{2+} mobilization on RhoA function.

Previous data from murine models indicate that RhoA, ROCK, and the actin cytoskeleton participate in stabilization of HIF-1α. Renal cortical tissue from diabetic *db*/*db* mice demonstrates increased Rho activity and HIF-1α protein compared to wild-type controls. Inhibition of ROCK in mesangial cells attenuated hypoxia-induced increases in HIF-1α and target gene expression by increasing PHD2 activity, thereby increasing HIF-1α hydroxylation and proteasomal degradation [32]. RhoA inhibition in trophoblasts prevents increased HIF-1α mRNA and protein expression in response to hypoxia or the hypoxia mimetic cobalt chloride [33]. Additional RhoA-based regulation of HIF-1α expression and HIF-alpha-dependent signaling has also been observed in endothelial [34] and ovarian cancer [35] cells. RhoA/ROCK-dependent regulation of HIF-1α appears to involve oxygen-sensitive (PHD2/Vhl) mechanisms, as increases in HIF-1α that normally occur with PHD inhibition by $CoCl_2$ were attenuated with the RhoA antagonist exoenzyme C3 transferase [33], and PHD2 expression decreases in the presence of the ROCK inhibitor fasudil [32]. Our data demonstrate that osteoblasts also regulate HIF-1α through a RhoA-dependent mechanism. PTH decreases actin polymerization [3] and HIF-1α (Fig. 1B), whereas induction of actin polymerization with LPA [36] increases pVEGF-Luc activity (Fig. 5B). This is likely mediated through Rho and its effector Rho kinase (ROCK), as exoenzyme C3 transferase, which inhibits RhoA/RhoB/RhoC, prevented LPA-induced increases in pVEGF-Luc activity (Fig. 5B). Further, direct activation of Rho through a pharmacologic agent that

prevents inherent GTPase activity [37] (Fig. 5C) and constitutively-active EGFP-RhoA-Q63L (Fig. 5D) each increased pVEGF-Luc activity.

PTH is critical for the anabolic effect of mechanical loading on the skeleton. Removal of parathyroid glands prevents load-induced bone formation, and responsiveness to loading is restored with acute injection of PTH [38]. Similarly, immobilization-induced bone loss is absent in animals lacking parathyroid glands [39]. It is believed that PTH, similar to estrogen, alters the mechanostat threshold at which loading induces an adaptive response, as acute PTH and mechanical loading produce synergistic responses [40,41] likely by altering the threshold at which mechanosensitive cation channels [4,5] and L-type voltage-sensitive calcium channels [4,41] activate. Because Riddle et al. have demonstrated that HIF-1α negatively regulates bone formation in response to mechanical loading [42], it is tempting to hypothesize that PTH alteration of the skeletal mechanostat involves suppression of HIF-1α. The in vitro work described within and the in vitro and in vivo results in Riddle et al. [42] and Wang et al. [10] were performed in osteoblastic cells, thus leading one to speculate whether the same holds true in osteocytes, which are the most numerous cell type within bone and are more ideally situated to perceive load-induced stress. Nonetheless, oxygen-independent regulation of HIF-1α and HIF-1α-driven gene expression is a novel effect of PTH in osteoblasts.

Supplementary Material

Refer to Web version on PubMed Central for supplementary material.

Acknowledgments

Research reported in this publication was supported by the National Institute of Arthritis and Musculoskeletal and Skin Diseases of the National Institutes of Health under award numbers R03AR057547 and R01AR064255 (DCG), and by the National Institute of Diabetes and Digestive and Kidney Diseases of the National Institutes of Health under award number R01DK075730 (GGL). The content is solely the responsibility of the authors and does not necessarily represent the official views of the National Institutes of Health. This work was performed under the auspices of the U.S. Department of Energy by Lawrence Livermore National Laboratory under Contract DE-AC52-07NA27344.

References

1. Augustine M, Horwitz MJ. Parathyroid hormone and parathyroid hormone-related protein analogs as therapies for osteoporosis. Curr. Osteoporos. Rep. 2013; 11:400–406. http://dx.doi.org/10.1007/s11914-013-0171-2. [PubMed: 24078470]
2. Babich M, Foti LR, Mathias KL. Protein kinase C modulator effects on parathyroid hormone-induced intracellular calcium and morphologic changes in UMR 106-H5 osteoblastic cells. J. Cell. Biochem. 1997; 65:276–285. [PubMed: 9136085]
3. Egan JJ, Gronowicz G, Rodan GA. Parathyroid hormone promotes the disassembly of cytoskeletal actin and myosin in cultured osteoblastic cells: mediation by cyclic AMP. J. Cell. Biochem. 1991; 45:101–111. http://dx.doi.org/10.1002/jcb.240450117. [PubMed: 1848561]
4. Ryder KD, Duncan RL. Parathyroid hormone enhances fluid shear-induced [Ca2+]i signaling in osteoblastic cells through activation of mechanosensitive and voltage-sensitive Ca2+ channels. J. Bone Miner. Res. 2001; 16:240–248. http:// dx.doi.org/10.1359/jbmr.2001.16.2.240. [PubMed: 11204424]
5. Zhang J, Ryder KD, Bethel JA, Ramirez R, Duncan RL. PTH-induced actin depolymerization increases mechanosensitive channel activity to enhance mechanically stimulated Ca2+ signaling in

osteoblasts. J. Bone Miner. Res. 2006; 21:1729–1737. http://dx.doi.org/10.1359/jbmr.060722. [PubMed: 17002579]

6. Li X, Liu H, Qin L, Tamasi J, Bergenstock M, Shapses S, et al. Determination of dual effects of parathyroid hormone on skeletal gene expression in vivo by microarray and network analysis. J. Biol. Chem. 2007; 282:33086–33097. http://dx.doi.org/10.1074/jbc.M705194200. [PubMed: 17690103]
7. Semenza GL. Hydroxylation of HIF-1: oxygen sensing at the molecular level. Physiology (Bethesda). 2004; 19:176–182. http://dx.doi.org/10.1152/physiol.00001.2004. [PubMed: 15304631]
8. Gerber HP, Vu TH, Ryan AM, Kowalski J, Werb Z, Ferrara N. VEGF couples hypertrophic cartilage remodeling, ossification and angiogenesis during endochondral bone formation. Nat. Med. 1999; 5:623–628. http://dx.doi.org/10.1038/9467. [PubMed: 10371499]
9. Huang Y-C, Kaigler D, Rice KG, Krebsbach PH, Mooney DJ. Combined angiogenic and osteogenic factor delivery enhances bone marrow stromal cell-driven bone regeneration. J. Bone Miner. Res. 2005; 20:848–857. http://dx.doi.org/10.1359/JBMR.041226. [PubMed: 15824858]
10. Wang Y, Wan C, Deng L, Liu X, Cao X, Gilbert SR, et al. The hypoxia-inducible factor alpha pathway couples angiogenesis to osteogenesis during skeletal development. J. Clin. Invest. 2007; 117:1616–1626. http://dx.doi.org/10.1172/JCI31581. [PubMed: 17549257]
11. Shomento SH, Wan C, Cao X, Faugere M-C, Bouxsein ML, Clemens TL, et al. Hypoxia-inducible factors 1alpha and 2alpha exert both distinct and overlapping functions in long bone development. J. Cell. Biochem. 2010; 109:196–204. http://dx.doi.org/10.1002/jcb.22396. [PubMed: 19899108]
12. Treins C, Giorgetti-Peraldi S, Murdaca J, Semenza GL, Van Obberghen E. Insulin stimulates HIF-1 through a PI-3-kinase/TOR-dependent pathway. J. Biol. Chem. 2002 http://dx.doi.org/10.1074/jbc.M204152200.
13. Treins C, Giorgetti-Peraldi S, Murdaca J, Monthouël-Kartmann M-N, Van Obberghen E. Regulation of hypoxia-inducible factor (HIF)-1 activity and expression of HIF hydroxylases in response to insulin-like growth factor I. Mol. Endocrinol. 2005; 19:1304–1317. http://dx.doi.org/10.1210/me.2004-0239. [PubMed: 15695372]
14. Slomiany MG, Rosenzweig SA. Hypoxia-inducible factor-1-dependent and -independent regulation of insulin-like growth factor-1-stimulated vascular endothelial growth factor secretion. J. Pharmacol. Exp. Ther. 2006; 318:666–675. http://dx.doi.org/10.1124/jpet.106.104158. [PubMed: 16682453]
15. Liu YV, Baek JH, Zhang H, Diez R, Cole RN, Semenza GL. RACK1 competes with HSP90 for binding to HIF-1alpha and is required for O(2)-independent and HSP90 inhibitor-induced degradation of HIF-1alpha. Mol. Cell. 2007; 25:207–217. http://dx.doi.org/10.1016/j.molcel.2007.01.001. [PubMed: 17244529]
16. Liu YV, Semenza GL. RACK1 vs. HSP90: competition for HIF-1 alpha degradation vs. stabilization. Cell Cycle. 2007; 6:656–659. [PubMed: 17361105]
17. Partridge NC, Alcorn D, Michelangeli VP, Ryan G, Martin TJ. Morphological and biochemical characterization of four clonal osteogenic sarcoma cell lines of rat origin. Cancer Res. 1983; 43:4308–4314. [PubMed: 6575864]
18. Lee CM, Genetos DC, You Z, Yellowley CE. Hypoxia regulates PGE(2) release and EP1 receptor expression in osteoblastic cells. J. Cell. Physiol. 2007; 212:182–188. http://dx.doi.org/10.1002/jcp.21017. [PubMed: 17370287]
19. Emerling BM, Weinberg F, Liu J-L, Mak TW, Chandel NS. PTEN regulates p300-dependent hypoxia-inducible factor 1 transcriptional activity through Forkhead transcription factor 3a (FOXO3a). Proc. Natl. Acad. Sci. U. S. A. 2008; 105:2622–2627. http://dx.doi.org/10.1073/pnas.0706790105. [PubMed: 18268343]
20. Roberts PJ, Mitin N, Keller PJ, Chenette EJ, Madigan JP, Currin RO, et al. Rho family GTPase modification and dependence on CAAX motif-signaled posttranslational modification. J. Biol. Chem. 2008; 283:25150–25163. http://dx.doi.org/10.1074/jbc.M800882200. [PubMed: 18614539]
21. Subauste MC, Herrath Von M, Benard V, Chamberlain CE, Chuang TH, Chu K, et al. Rho family proteins modulate rapid apoptosis induced by cytotoxic T lymphocytes and Fas. J. Biol. Chem. 2000; 275:9725–9733. [PubMed: 10734125]

22. Isaacs JS, Jung Y-J, Mimnaugh EG, Martinez A, Cuttitta F, Neckers LM. Hsp90 regulates a von Hippel Lindau-independent hypoxia-inducible factor-1 alpha-degradative pathway. J. Biol. Chem. 2002; 277:29936–29944. http://dx.doi.org/10.1074/jbc.M204733200. [PubMed: 12052835]
23. Bucci M, Roviezzo F, Cicala C, Sessa WC, Cirino G. Geldanamycin, an inhibitor of heat shock protein 90 (Hsp90) mediated signal transduction has anti-inflammatory effects and interacts with glucocorticoid receptor in vivo. Br. J. Pharmacol. 2000; 131:13–16. http://dx.doi.org/10.1038/sj.bjp.0703549. [PubMed: 10960063]
24. Fujimori A, Cheng SL, Avioli LV, Civitelli R. Structure-function relationship of parathyroid hormone: activation of phospholipase-C, protein kinase-A and -C in osteosarcoma cells. Endocrinology. 1992; 130:29–36. http://dx.doi.org/10.1210/endo.130.1.1727705. [PubMed: 1727705]
25. Semenza GL. Hypoxia-inducible factor 1 (HIF-1) pathway. Sci. STKE. 2007; 2007 cm8-cm8, http://dx.doi.org/10.1126/stke.4072007cm8.
26. Zhang D, Li J, Costa M, Gao J, Huang C. JNK1mediates degradation HIF-1alpha by a VHL-independent mechanism that involves the chaperones Hsp90/Hsp70. Cancer Res. 2010; 70:813–823. http://dx.doi.org/10.1158/0008-5472.CAN-09-0448. [PubMed: 20068160]
27. Egan JJ, Gronowicz G, Rodan GA. Cell density-dependent decrease in cytoskeletal actin and myosin in cultured osteoblastic cells: correlation with cyclic AMP changes. J. Cell. Biochem. 1991; 45:93–100. http://dx.doi.org/10.1002/jcb.240450116. [PubMed: 1848564]
28. Dong JM, Leung T, Manser E, Lim L. cAMP-induced morphological changes are counteracted by the activated RhoA small GTPase and the Rho kinase ROKalpha. J. Biol. Chem. 1998; 273:22554–22562. [PubMed: 9712882]
29. Radeff JM, Nagy Z, Stern PH. Rho and Rho kinase are involved in parathyroid hormone-stimulated protein kinase C alpha translocation and IL-6 promoter activity in osteoblastic cells. J. Bone Miner. Res. 2004; 19:1882–1891. http://dx.doi.org/10.1359/JBMR.040806. [PubMed: 15476589]
30. Singh ATK, Gilchrist A, Voyno-Yasenetskaya T, Radeff-Huang JM, Stern PH. G alpha12/G alpha13 subunits of heterotrimeric G proteins mediate parathyroid hormone activation of phospholipase D in UMR-106 osteoblastic cells. Endocrinology. 2005; 146:2171–2175. http://dx.doi.org/10.1210/en.2004-1283. [PubMed: 15705779]
31. Kazmers NH, Ma SA, Yoshida T, Stern PH. Rho GTPase signaling and PTH 3–34, but not PTH 1–34, maintain the actin cytoskeleton and antagonize bisphosphonate effects in mouse osteoblastic MC3T3-E1 cells. Bone. 2009; 45:52–60. http://dx.doi.org/10.1016/j.bone.2009.03.675. [PubMed: 19361585]
32. Matoba K, Kawanami D, Okada R, Tsukamoto M, Kinoshita J, Ito T, et al. Rho-kinase inhibition prevents the progression of diabetic nephropathy by downregulating hypoxia-inducible factor 1. Kidney Int. 2013; 84:545–554. http://dx.doi.org/10.1038/ki.2013.130. [PubMed: 23615507]
33. Hayashi M, Sakata M, Takeda T, Tahara M, Yamamoto T, Minekawa R, et al. Hypoxia Up-Regulates Hypoxia-Inducible Factor-1α Expression through RhoA Activation in Trophoblast Cells. 2013 http://dx.doi.org/10.1210/jc.2004-1547.
34. Takata K, Morishige K-I, Takahashi T, Hashimoto K, Tsutsumi S, Yin L, et al. Fasudil-induced hypoxia-inducible factor-1alpha degradation disrupts a hypoxia-driven vascular endothelial growth factor autocrine mechanism in endothelial cells. Mol. Cancer Ther. 2008; 7:1551–1561. http://dx.doi.org/10.1158/1535-7163.MCT-07-0428. [PubMed: 18566226]
35. Ohta T, Takahashi T, Shibuya T, Amita M. Inhibition of the Rho/ROCK pathway enhances the efficacy of cisplatin through the blockage of hypoxia-inducible factor-1α in human ovarian cancer cells. Cancer Biol. 2012
36. Masiello LM, Fotos JS, Galileo DS, Karin NJ. Lysophosphatidic acid induces chemotaxis in MC3T3-E1 osteoblastic cells. Bone. 2006; 39:72–82. http://dx.doi.org/10.1016/j.bone.2005.12.013. [PubMed: 16487757]
37. Flatau G, Lemichez E, Gauthier M, Chardin P, Paris S, Fiorentini C, et al. Toxin-induced activation of the G protein p21 Rho by deamidation of glutamine. Nature. 1997; 387:729–733. http://dx.doi.org/10.1038/42743. [PubMed: 9192901]

38. Chow JW, Fox S, Jagger CJ, Chambers TJ. Role for parathyroid hormone in mechanical responsiveness of rat bone. Am. J. Physiol. 1998; 274:E146–E154. [PubMed: 9458760]

39. Burkhart JM, Jowsey J. Parathyroid and Thyroid Hormones in the development of immobilization osteoporosis. Endocrinology. 1967; 81:1053–1062. http://dx.doi.org/10.1210/endo-81-5-1053. [PubMed: 6052936]

40. Ma Y, Jee WSS, Yuan Z, Wei W, Chen H, Pun S, et al. Parathyroid hormone and mechanical usage have a synergistic effect in rat tibial diaphyseal cortical bone. J. Bone Miner. Res. 1999; 14:439–448. http://dx.doi.org/10.1359/jbmr.1999.14.3.439. [PubMed: 10027909]

41. Li J, Duncan RL, Burr DB, Gattone VH, Turner CH. Parathyroid hormone enhances mechanically induced bone formation, possibly involving L-type voltage-sensitive calcium channels. Endocrinology. 2003; 144:1226–1233. [PubMed: 12639904]

42. Riddle RC, Leslie JM, Gross TS, Clemens TL. Hypoxia-inducible factor-1α protein negatively regulates load-induced bone formation. J. Biol. Chem. 2011; 286:44449–44456. http://dx.doi.org/10.1074/jbc.M111.276683. [PubMed: 22081627]

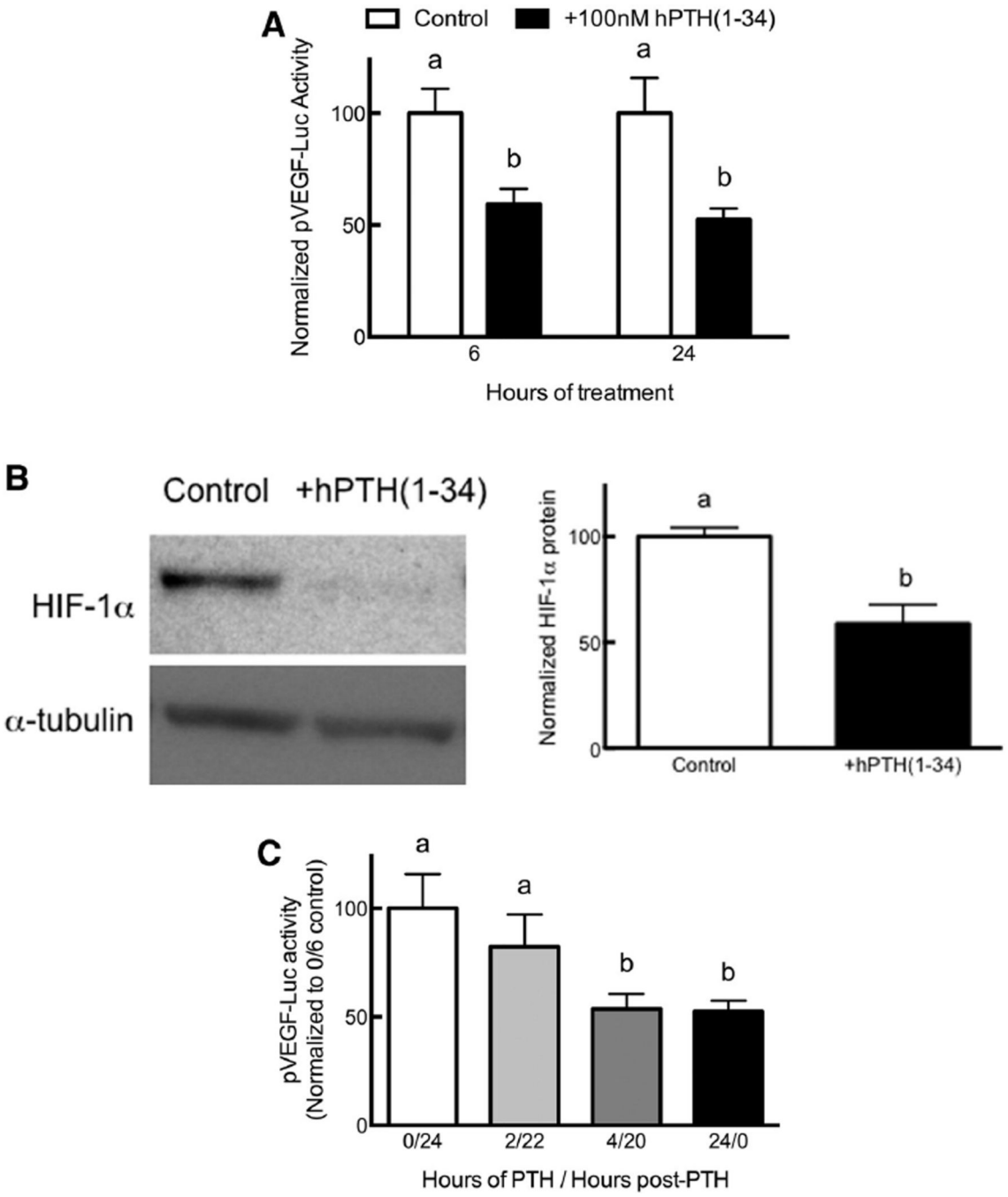

Fig. 1.

PTH(1–34) rapidly decreases HIF-1α-driven transcription and protein expression. (A) pVEGF-Luc-transfected UMR 106.01 osteoblasts reveal decreased luciferase activity in response to hPTH(1–34) for 6 or 24 h. (B) HIF-1α protein level decreases in response to 24 h hPTH(1–34) without affecting α-tubulin. (C) Quantification of HIF-1α protein relative to α-tubulin protein in response to 24 h of control or hPTH(1–34). (D) hPTH(1–34) decreases luciferase activity in an unrelated HRE-containing plasmid, pPGK1-Luc. (E) pVEGF-Luc-transfected UMR106.01 osteoblasts indicate that duration of hPTH(1–34) exposure sustains

pVEGF-Luc suppression (n = 3–5 per experiment). Groups with different letters are statistically different from each other, $p < 0.05$.

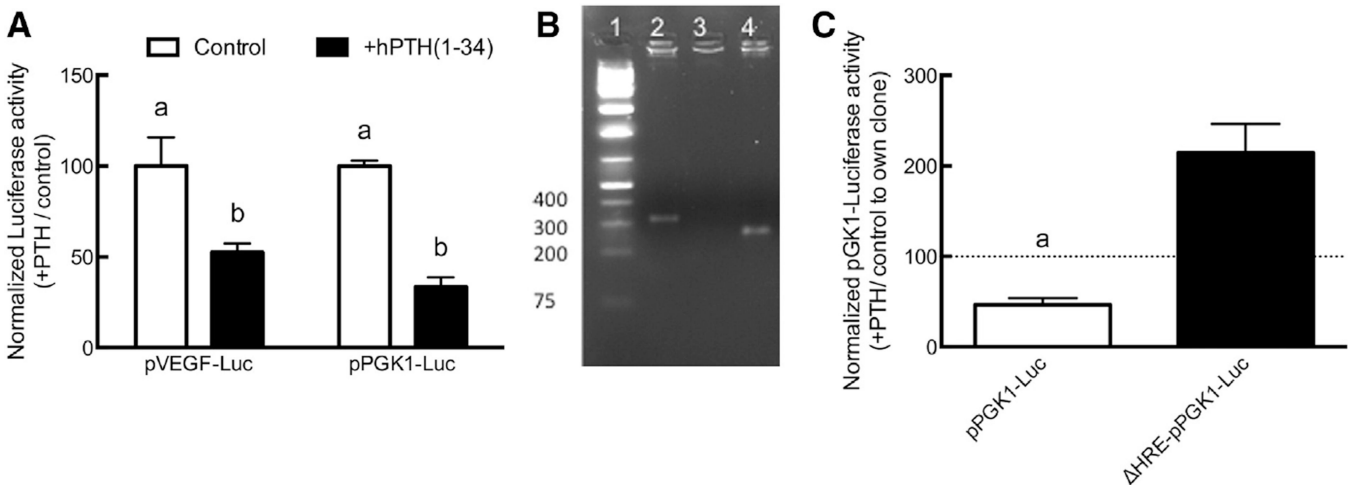

Fig. 2.

PTH(1–34) specifically targets the HRE in reporter plasmids. (A) pPGK1-Luc-transfected and pVEGF-Luc osteoblasts show similar suppressive effect of luciferase activity in response to hPTH(1–34). (B) PCR analysis of parental and HRE-deleted pPGK1-Luc plasmids. (C) Deletion of HRE elements in pPGK1-Luc eliminates the suppressive effect of PTH on luciferase activity. (n= 3–4 per experiment). Groups with different letters are statistically different from each other, $p < 0.05$.

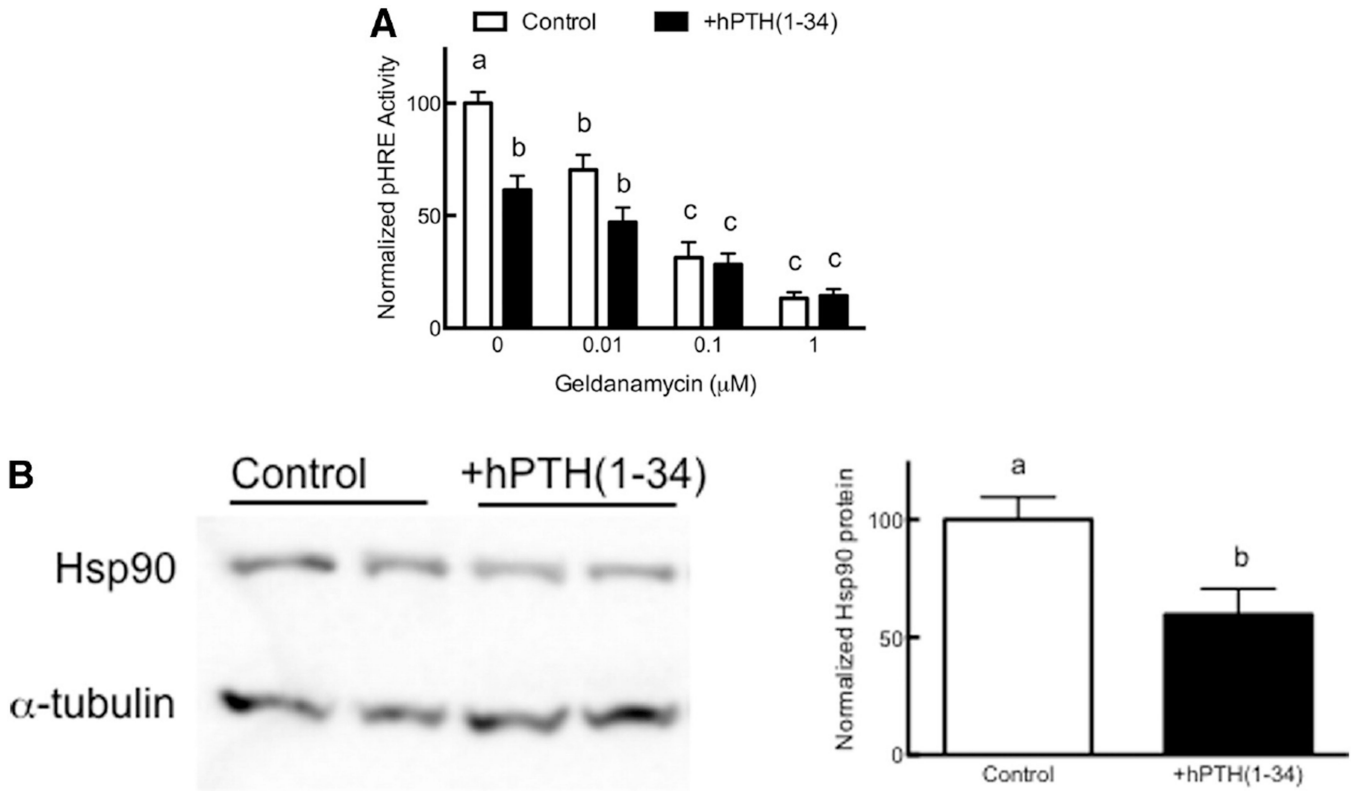

Fig. 3.

Hsp90 is involved in oxygen-independent HIF-1α stabilization and is decreased by hPTH(1–34). (A) The Hsp90 antagonist geldanamycin dose-dependently decreases pVEGF-Luc activity in transfected osteoblasts. (B) Lack of synergistic effect of hPTH(1–34) and geldanamycin on pVEGF-Luc activity in osteoblasts. (C) Hsp90 protein expression decreases in response to 24 h hPTH(1–34) treatment compared to vehicle-treated controls (n = 4–6 per experiment). Groups with different letters are statistically different from each other, $p < 0.05$.

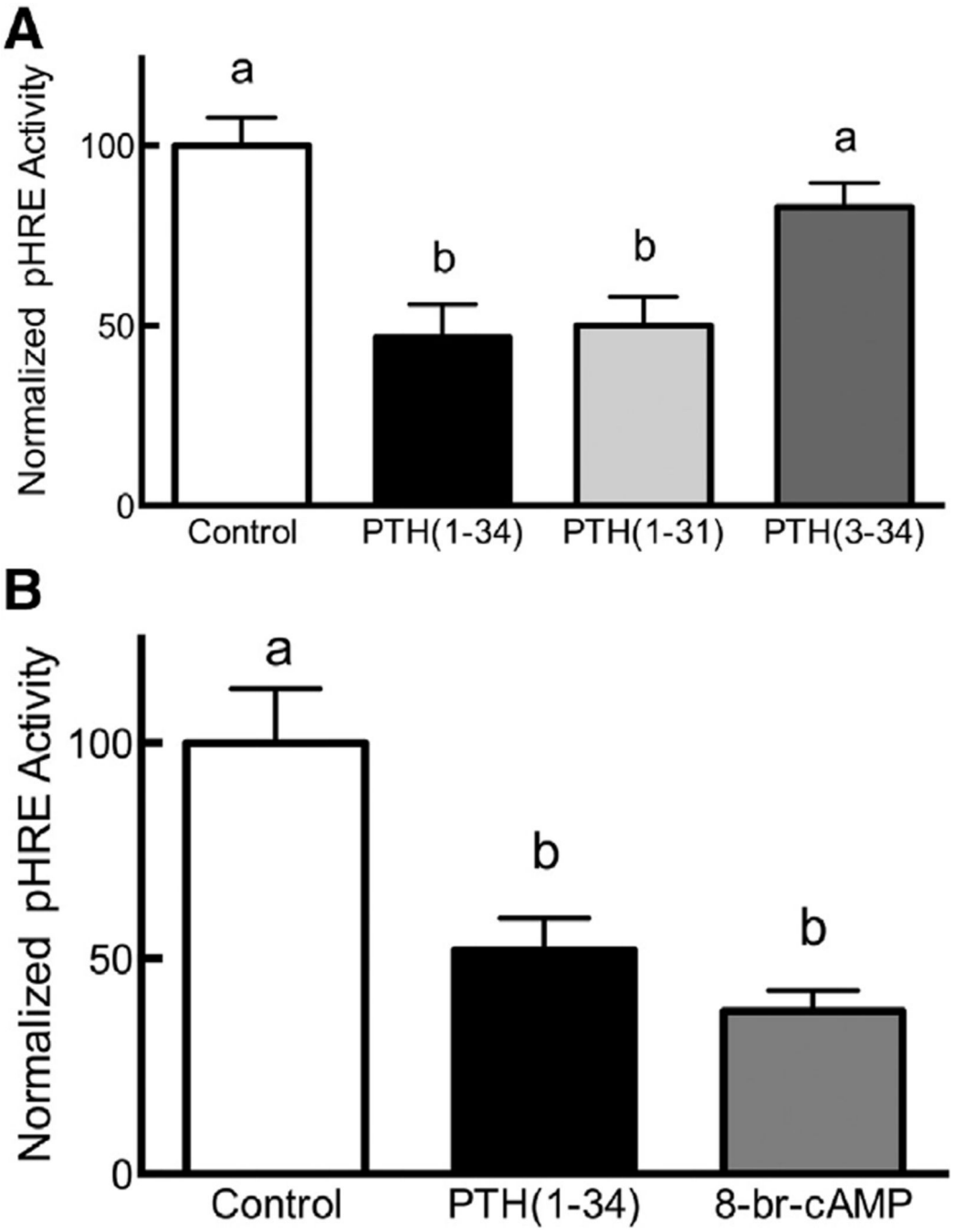

Fig. 4.

hPTH(1–34) decreases pVEGF-Luc through cAMP. (A) 100 nM hPTH(1–34) and hPTH(1–31), but not bPTH(3–34), decrease pVEGF-Luc. (B) hPTH(1–34) suppressive effects on pVEGF-Luc are mimicked by 1 mM 8-br-cAMP (n = 3). Groups with different letters are statistically different from each other, $p < 0.05$.

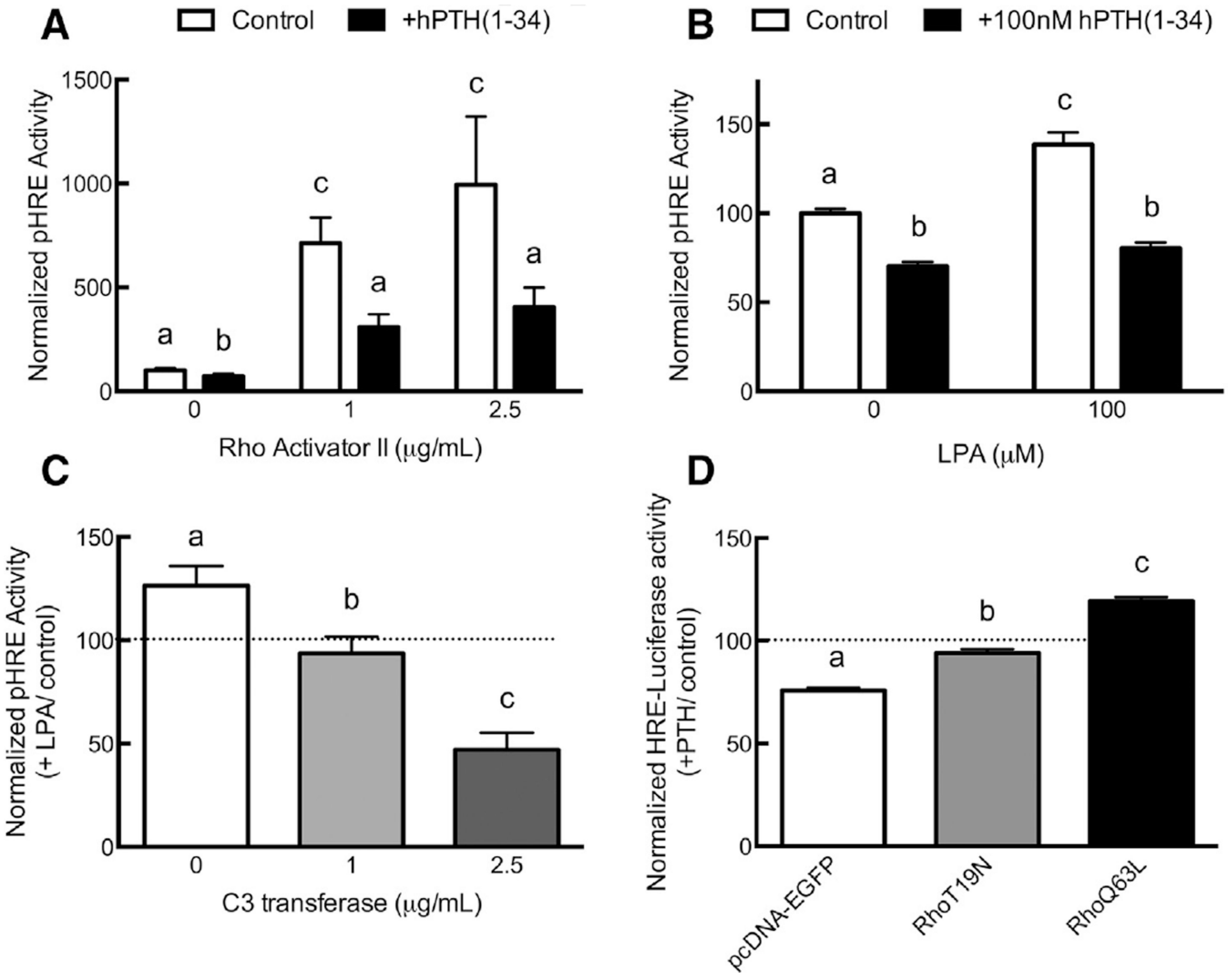

Fig. 5.

Involvement of RhoA in PTH regulation of pVEGF-Luc activity. (A) LPA (100 μM) increases pVEGF-Luc activity inUMR106.01 osteoblasts which is inhibited by 100 nM hPTH(1–34). (B) Inhibition of RhoA dose-dependently decreases 100 μM LPA-stimulated pVEGF-Luc activity. (C) Direct activation of RhoA by Rho Activator II increases pVEGF-Luc activity and is decreased by hPTH(1–34). (D) Compared to cells transfected with control plasmid pcDNA-EGFP and treated with hPTH(1–34), cells transfected with dominant negative RhoA EGFP-RhoA-T19N show no effect of PTH(1–34) on pVEGF-Luc while cells transfected with constitutively active EGFP-RhoA-Q63L lose the suppressive effect of PTH on pVEGF-Luc. Groups with different letters are statistically different from each other.